Both probes hybridized to the transcripts of *Pp1α-96A* [2.3 kb (*26*)] and *rox8* [3 to 3.3 kb (*11*)] only, and no detectable differences in the expression of these genes between st-1 and j-1 were observed. It seems that inversion *2j* neither disrupted any transcriptional unit nor affected the expression of the closest genes, ruling out a relation between the mutational effect of the inversion and its adaptive value (*29*).

References and Notes

1. C. B. Krimbas and J. R. Powell, Eds., Drosophila *Inversion Polymorphism* (CRC Press, Boca Raton, FL, 1992).
2. J. R. Powell, *Progress and Prospects in Evolutionary Biology: The* Drosophila *Model* (Oxford Univ. Press, New York, 1997).
3. W. R. Engels and C. R. Preston, *Genetics* **107**, 657 (1984); S. Schneuwly, A. Kuroiwa, W. J. Gehring, *EMBO J.* **6**, 201 (1987); E. A. Montgomery, S.-M. Huang, C. H. Langley, B. H. Judd, *Genetics* **129**, 1085 (1991); J. K. Lim and M. J. Simmons, *Bioessays* **16**, 269 (1994); V. Ladeveze, S. Aulard, N. Chaminade, G. Periquet, F. Lemeunier, *Proc. R. Soc. London Ser. B* **265**, 1157 (1998).
4. T. W. Lyttle and D. S. Haymer, *Genetica* **86**, 113 (1992).
5. C. S. Wesley and W. F. Eanes, *Proc. Natl. Acad. Sci. U.S.A.* **91**, 3132 (1994); S. Cirera, J. M. Martín-Campos, C. Segarra, M. Aguadé, *Genetics* **139**, 321 (1995).
6. M. Wasserman, in (*7*), pp. 455–541; A. Ruiz and M. Wasserman, *Heredity* **70**, 582 (1993).
7. A. Fontdevila, A. Ruiz, G. Alonso, J. Ocaña, *Evolution* **35**, 148 (1981); A. Ruiz, H. Naveira, A. Fontdevila, *Genet. Iber.* **36**, 13 (1984); E. Hasson *et al.*, *J. Evol. Biol.* **8**, 369 (1995).
8. J. M. Ranz, C. Segarra, A. Ruiz, *Genetics* **145**, 281 (1997); J. M. Ranz, M. Cáceres, A. Ruiz, *Chromosoma* **108**, 32 (1999).
9. E. Sawruk, C. Udri, H. Betz, B. Schmitt, *FEBS Lett.* **273**, 177 (1990).
10. For the construction of genomic libraries, ~30 μg of high molecular weight genomic DNA were partially digested with Sau 3AI and electrophoresed on a 0.4% agarose gel. Fragments in the size range 15 to 23 kb were eluted from the gel, ligated with LambdaGEM-11 Bam HI arms, and packaged in vitro using Packagene extracts (Promega).
11. S. Brand and H.-M. Bourbon, *Nucleic Acids Res.* **21**, 3699 (1993).
12. I. Busseau, A. Pelisson, A. Bucheton, *Mol. Gen. Genet.* **218**, 222 (1989); N. Nassif and W. R. Engels, *Proc. Natl. Acad. Sci. U.S.A.* **90**, 1262 (1993).
13. D. J. Finnegan, *Trends Genet.* **5**, 103 (1989); P. Capy, C. Bazin, D. Higuet, T. Langin, *Dynamics and Evolution of Transposable Elements* (Springer-Verlag, Heidelberg, 1998).
14. The insertions at the *2j* inversion breakpoints do not show homology at the nucleotide level to any known sequence in the databases and thus appear to correspond to a previously undescribed TE. We have named this TE after the Italian astronomer, mathematician, and physicist Galileo Galilei (1564–1642).
15. A 5-kb probe of the λj3.1 proximal end that contains most of the *BD* insertion was in situ hybridized to the polytene chromosomes of seven *D. buzzatii* lines. The total number of euchromatic signals found per genome was 55 in st-1, 44 in st-3, 47 in st-4, 34 in j-1, 34 in j-8, 37 in j-11, and 28 in j-13 (*23*). On average, 11.8% of each line's signals were exclusive.
16. K. O'Hare and G. M. Rubin, *Cell* **34**, 25 (1983); R. D. Streck, J. E. MacGaffey, S. K. Beckendorf, *EMBO J.* **5**, 3615 (1986).
17. I. Marín and A. Fontdevila, *Mol. Gen. Genet.* **248**, 423 (1995).
18. G. S. Roeder and G. R. Fink, in *Mobile Genetic Elements*, J. Shapiro, Ed. (Academic Press, Orlando, FL, 1983), pp. 299–328; T. D. Petes and C. W. Hill, *Annu. Rev. Genet.* **22**, 147 (1988).
19. D. Lakich, H. H. Kazazian, S. E. Antonarakis, J. Gitschier, *Nature Genet.* **5**, 236 (1993); J. A. Naylor *et al.*, *Hum. Mol. Genet.* **4**, 1217 (1995); K. Small, J. Iber, S. T. Warren, *Nature Genet.* **16**, 96 (1997).
20. W. B. Eggleston, N. R. Rim, J. K. Lim, *Genetics* **144**, 647 (1996).
21. Y. Komoda, M. Enomoto, A. Tominaga, *ibid.* **129**, 639 (1991); M.-L. Daveran-Mingot, N. Campo, P. Ritzenthaler, P. le Bourgeois, *J. Bacteriol.* **180**, 4834 (1998).
22. K. D. Mathiopoulos, A. della Torre, V. Predazzi, V. Petrarca, M. Coluzzi, *Proc. Natl. Acad. Sci. U.S.A.* **95**, 12444 (1998).
23. The *D. buzzatii* lines used are homokaryotypic for four different chromosome arrangements: *2st*, *2j*, $2jz^3$, and $2jq^7$ ($2jz^3$ and $2jq^7$ derive from the *2j* arrangement and bear inversions $2z^3$ and $2q^7$, respectively). Their geographic origins cover a major part of the species distribution; lines that were sequenced are indicated in boldface. Spain: **st-1**, st-2, **j-1**, j-2, j-3, j-4, j-5, j-6, jz^3-1, jz^3-2, and jq^7-1 (Carboneras), j-7 and jq^7-3 (Caldetas), and jq^7-2 (Mogan, Canary Islands). Tunisia: jz^3-3 (Kariouan). Argentina: **st-3** (Vipos), **j-8** (San Luis), j-9 (Quilmes), j-10 (Palo Labrado), and jq^7-4 (Otamendi). Bolivia: **j-11** (Los Negros). Brazil: **st-4**, **j-12**, and j-13 (Guaritas, RS). Australia: **j-14**. All lines (except jq^7-3 and jq^7-4) were made isogenic by repeated sib-mating or by using the second chromosome balancer stock *Antp*/Δ*5* [J. S. F. Barker, *Genetica* **92**, 165 (1994)].
24. The PCR products were purified from 1% agarose gels, reamplified with one of the sequencing primers shown in Fig. 2, and sequenced in an ALFexpress DNA automated sequencer (Pharmacia Biotech). Both strands of each fragment were sequenced completely using primers separated by 323 to 466 nucleotides.
25. M. Nei, *Molecular Evolutionary Genetics* (Columbia Univ. Press, New York, 1987).
26. V. Dombrádi *et al.*, *Eur. J. Biochem.* **194**, 739 (1990).
27. Two sets of primers were used to amplify simultaneously a 271-bp 5′ fragment of the *Pp1α-96A* cDNA and 438 bp of the *Gapdh* cDNA (internal control) from the total cDNA. In both cases the primer sites were selected to span introns (of 61 bp and 69 bp, respectively). *Gapdh* primers were designed on the basis of the sequence of *D. hydei* [K. M. Wojtas, L. von Kalm, J. R. Weaver, D. T. Sullivan, *Genetics* **132**, 789 (1992)]. PCRs were performed with varying amounts of the reverse transcription reaction product as template and different concentrations of the two sets of primers.
28. The Northern blot hybridization was done with ~30 μg of total RNA from embryos, larvae, pupae, and adults of the st-1 and j-1 lines as described [A.-K. Rost, in *Quantitation of mRNA by Polymerase Chain Reaction: Nonradioactive PCR Methods*, Th. Köhler *et al.*, Eds. (Springer-Verlag, Berlin, 1995), pp. 93–114].
29. A. Ruiz *et al.*, *Genetics* **128**, 739 (1991); E. Betrán, M. Santos, A. Ruiz, *Evolution* **52**, 144 (1998).
30. W. R. Engels, D. M. Johnson-Schlitz, W. B. Eggleston, J. Sved, *Cell* **62**, 515 (1990); R. H. A. Plasterk, *EMBO J.* **10**, 1919 (1991); E. Takasu-Ishikawa, M. Yoshihara, Y. Hotta, *Mol. Gen. Genet.* **232**, 17 (1992).

31. Supported by a doctoral fellowship and a travel grant from the Comissionat per a Universitats i Recerca (Generalitat de Catalunya, Spain) (M.C.) and grant PB95-0607 from the Dirección General de Investigación Científica y Técnica (Ministerio de Educación y Cultura, Spain) (A.R.). We thank J. Zhang for his help in the RNA work; J. Barbé, O. Cabré, and A. Tapias for material and technical help; B. Schmitt for the *nAcRβ-96A* clone; J. S. F. Barker, E. Betrán, A. Fontdevila, and F. M. Sene for *D. buzzatii* stocks; and M. Aguadé, M. Ashburner, A. Berry, F. Brunet, B. Charlesworth, and R. de Frutos for valuable comments and helpful discussions.

4 February 1999; accepted 9 June 1999

Identification of a Vertebrate Sister-Chromatid Separation Inhibitor Involved in Transformation and Tumorigenesis

Hui Zou, Thomas J. McGarry, Teresita Bernal, Marc W. Kirschner*

A vertebrate securin (vSecurin) was identified on the basis of its biochemical analogy to the Pds1p protein of budding yeast and the Cut2p protein of fission yeast. The vSecurin protein bound to a vertebrate homolog of yeast separins Esp1p and Cut1p and was degraded by proteolysis mediated by an anaphase-promoting complex in a manner dependent on a destruction motif. Furthermore, expression of a stable *Xenopus* securin mutant protein blocked sister-chromatid separation but did not block the embryonic cell cycle. The vSecurin proteins share extensive sequence similarity with each other but show no sequence similarity to either of their yeast counterparts. Human securin is identical to the product of the gene called pituitary tumor-transforming gene (*PTTG*), which is overexpressed in some tumors and exhibits transforming activity in NIH 3T3 cells. The oncogenic nature of increased expression of vSecurin may result from chromosome gain or loss, produced by errors in chromatid separation.

The metaphase to anaphase transition is the final discrete event in duplication and separation of the genetic material of a cell. Its timing is regulated by the activation of the anaphase-promoting complex (APC), which mediates selective proteolysis of various mitotic regulators (*1*–*3*). Experiments with *Xenopus* egg extracts indicated that a putative protein factor might exist whose degradation was required for the onset of sister-chromatid separation (*4*). Proteins with such an activity

Department of Cell Biology, Harvard Medical School, 240 Longwood Avenue, Boston, MA 02115, USA.

*To whom correspondence should be addressed. E-mail: marc@hms.harvard.edu

were subsequently found in both budding yeast and fission yeast, encoded by the genes *PDS1* and *CUT2*, respectively (*5–7*). Both proteins are APC substrates and their degradation is required for chromatid separation (*8, 9*). Pds1p and Cut2p associate with the yeast separin proteins Esp1p and Cut1p, respectively (*10, 11*), and prevent the separins from promoting chromatid separation. Because of their similar cell cycle functions, Pds1p and Cut2p are also called anaphase inhibitors or securins (*12*).

The regulation of sister-chromatid separation in metazoans might be similar. Unfortunately, Pds1p and Cut2p show no sequence similarity to each other, and currently no sequence in the GenBank and EST databases shows any similarity to either of them. The COOH-terminus of a putative human separin homolog (hESP1), found by cDNA sequencing (*13*), has 28% identity with budding yeast Esp1p and 30% identity with fission yeast Cut1p (*11*). There is no similarity in the NH_2-terminus. We therefore attempted to identify the human securin homolog through its expected association with the putative human separin.

Antibodies to hESP1 were raised to a 269–amino acid fragment at the COOH-terminal region of hESP1 (*14*). After affinity purification, the antibodies were covalently coupled to protein A beads (*15*). Using these antibodies, we looked for proteins that coimmunoprecipitated with hESP1 proteins that were present in extracts of cells in metaphase but not in extracts of cells in anaphase, the expected properties of a human securin homolog. These extracts were prepared by release of human HeLa S3 cells from nocodazole-induced metaphase arrest (*16*). At various times, extracts were prepared and immunoprecipitated with anti-hESP1 (*17*). Immunoprecipitated proteins were separated by SDS–polyacrylamide gel electrophoresis (PAGE) and detected by silver staining. Among the many proteins that immunoprecipitated, two had apparent molecular sizes of 28 kD (EAP1, for hESP1-associated protein 1) and 42 kD (EAP2, for hESP1-associated protein 2). Both proteins were present in constant amounts in extracts prepared at various times up to 90 min after removing nocodazole. Neither protein was present in extracts prepared 4 hours after release from metaphase arrest (Fig. 1A). As a temporal control for progress through M phase, amounts of cyclin B1 were monitored by protein immunoblot analysis. Like EAP1 and EAP2, cyclin B1 was stable up to 90 min after release but was not detected at the 4-hour time point (Fig. 1A), indicating that the APC-mediated proteolysis pathway became active between 90 min and 4 hours after release. The coincidence between the loss of association of EAP1 and EAP2 with hESP1 and the activation of APC suggests that EAP1 and EAP2 could be candidates for a human securin-like molecule.

We had also isolated *Xenopus* APC substrates by small-pool expression cloning (*18, 19*). In this approach, small pools of cDNA clones from a *Xenopus* blastula library (*20*) were translated and labeled in vitro in rabbit reticulocyte lysates. Each pool was divided and incubated in mitotic extract or interphase extract. The cDNA clones corresponding to proteins that were proteolyzed in mitotic extract but not in interphase extract were isolated. We identified various cyclin Bs and geminin, an inhibitor of DNA replication degraded upon exit from mitosis (*19*). Two other proteins were identified in this screen: a 70-kD kinesin-like protein and a 25-kD protein (p25). The primary structure of *Xenopus* p25 shares extensive similarity with a human protein encoded by a gene called pituitary tumor-transforming gene (*PTTG*) (*21–23*). The open reading frame of *PTTG* from a human fetal thymus cDNA library was isolated and antibody to full-length PTTG protein was prepared (*14*). The following evidence suggested that EAP1 might be identical to PTTG. First, in vitro–translated PTTG protein migrated with the same mobility as EAP1 on SDS-PAGE (*24*). Second, PTTG also associated with hESP1. Endogenous PTTG coimmunoprecipitated with antibody to hESP1 in HeLa cell extract as detected by the antibody to PTTG (Fig. 1B). Endogenous hESP1 also coimmunoprecipitated with antibody to the Myc tag in extracts prepared from 293T cells transiently expressing Myc-tagged PTTG (Fig. 1C). Furthermore, hESP1 and PTTG from HeLa cell extracts cofractionated on both anionic exchange (*24*) and gel filtration columns (Fig. 1D). Thus, PTTG appears to be a vertebrate APC substrate that is associated with a vertebrate separin until activation of the APC. Therefore, we tentatively

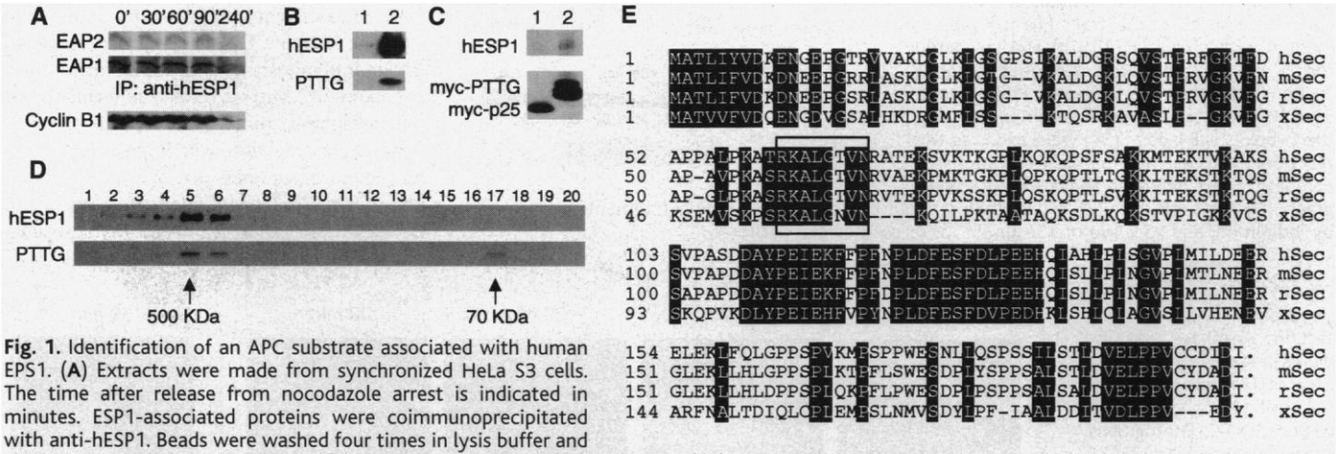

Fig. 1. Identification of an APC substrate associated with human EPS1. (**A**) Extracts were made from synchronized HeLa S3 cells. The time after release from nocodazole arrest is indicated in minutes. ESP1-associated proteins were coimmunoprecipitated with anti-hESP1. Beads were washed four times in lysis buffer and proteins were analyzed by SDS-PAGE. The amounts of cyclin B1 were determined by protein immunoblotting. (**B**) Immunoprecipitation with anti-hESP1 from extracts of HeLa S3 cells. As a control, preimmune antiserum (lane 1) was used in parallel with anti-hESP1 (lane 2). Both hESP1 and PTTG were detected by protein immunoblotting with respective antibodies. (**C**) Immunoprecipitations with antibody to the Myc tag (Santa Cruz) were performed in extracts prepared form 293T cells transfected with either Myc-tagged human PTTG (lane 2) or Myc-tagged *Xenopus* p25 (lane 1). Protein immunoblotting was performed to detect hESP1. We were unable to immunoprecipitate hESP1 with antibody to full-length PTTG, presumably because the binding sites on PTTG for ESP1 and the antibody overlap. (**D**) The fractions from a Superdex 200 column (*33*) were analyzed by protein immunoblotting to detect hESP1 and PTTG. Most of the PTTG cofractionated with hESP1 at an apparent molecular size of ~500 kD. Some PTTG was detected in fractions corresponding to ~70 kD, the same elution position of recombinant PTTG protein (*24*). (**E**) Sequence alignment of vertebrate securins (*25*). The hSecurin h(Sec) sequence obtained in this study (*14*) is identical to that of the human PTTG (*21*). The sequences of mouse securin (mSec) and rat securin (rSec) were obtained from GenBank (accession numbers AF069051 and U73030, respectively) (xSec, *Xenopus* securin). Amino acid sequence alignment was obtained with MegaAlign (DNAStar) by the clustal method. Residues that are identical or conserved among all four proteins are shaded in black. The conserved D-box is boxed.

named EAP1/PTTG as hSecurin and *Xenopus* p25 as xSecurin.

Among the vertebrate securins, sequence similarity was observed throughout the entire sequence (Fig. 1E). A conserved motif [RKALG(T or N)VN] (*25*) matches the destruction box (D-box) [RX(A or V or T)LGXXXN] shared by many APC substrates (*26*). The vertebrate securins share no sequence similarity with their yeast counterparts. In fact, the frog securin displays unusual diversity from its mammalian homologs (about 30% identity); most other cell cycle proteins are more than 80% identical in sequence. Nonetheless, there are conserved sequence features shared by all securins. All securins contain clusters of acidic and basic domains. The NH_2-terminal half of the proteins is rich in lysine residues surrounding the D-box. This is common for D-box–containing APC substrates, presumably because lysine is the residue that forms a covalent isopeptide linkage with ubiquitin.

To characterize the cell cycle function of vertebrate securins, we determined their abundance at various stages of the cell cycle. HeLa S3 cells were synchronized by release from a double-thymidine block, and extracts were prepared during the following 12 hours. Securin was detected by anti-hSecurin as two closely spaced bands. The amount of securin begins to accumulate at the onset of S phase and peaks at G_2-M phases in parallel with cyclin B1. As expected, its level drops precipitously when APC is activated, indicated by the decline of cyclin B1 (Fig. 2A).

Genetic studies in yeast and biochemical experiments in *Xenopus* egg extracts using yeast Pds1p and Cut2p suggested that Pds1p and Cut2p are ubiquitinated by the APC in a D-box–dependent manner (*8, 27*). To determine whether the putative D-box of the vertebrate securin is functional, we mutated the RKAL residues to AKAA (*25*) by site-directed mutagenesis. Mutated xSecurin (xSecurin^{dm}) was stable in mitotic extracts, confirming that the RKAL sequence is required for degradation (Fig. 2B). Similar observations were made with hSecurin (*24*). Furthermore, xSecurin was stabilized in the presence of an excess of an NH_2-terminal fragment of cyclin B1 that contains a D-box. However, the same cyclin B1 fragment lacking a D-box motif did not affect the degradation of xSecurin (Fig. 2C). Conversely, an excess of wild-type xSecurin, but not xSecurin^{dm}, inhibited the degradation of cyclin B1 (Fig. 2D). Taken together, these results demonstrate that the abundance of xSecurin is regulated by APC-mediated proteolysis in a D-box–dependent manner.

In yeast, the securins (Pds1p and Cut2p) function as inhibitors of chromatid separation. We therefore tested the effects of xSecurin^{dm} on sister-chromatid separation in *Xenopus* egg extracts (*4, 28*). In these experiments, we allowed extracts to go through one full cell cycle and observed chromatid separation at the following anaphase. Approximately 1 μl of purified xSecurin^{dm} protein (0.5 mg/ml) was added with *Xenopus* sperm nuclei and rhodamine tubulin to a 10-μl portion of a freshly prepared egg extract arrested at a metaphase-like stage (unfertilized egg extract). For comparison, equal amounts of bovine serum albumin were added to a separate sample of the same extract. The extracts were released into interphase by addition of calcium to allow DNA replication and then driven into mitosis by addition of unfertilized egg extract (2.5 μl) to allow the formation of the metaphase spindle. To prevent chromosome decondensation, which makes detection of the chromosomes difficult at late anaphase, we also added a nondegradable cyclin B1 lacking the NH_2-terminal 90 amino acids

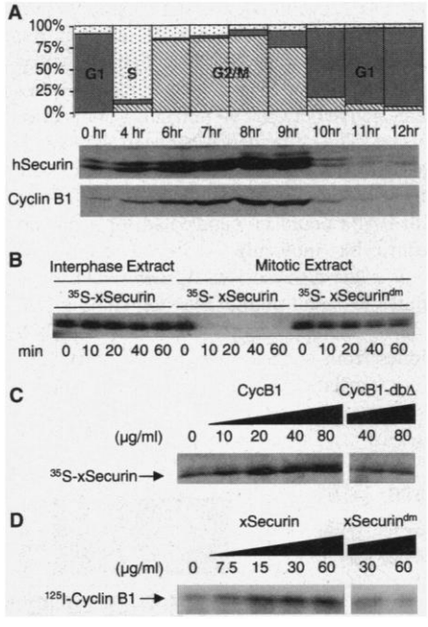

Fig. 2. Degradation of the vertebrate homolog of Pds1p by APC-mediated proteolysis. **(A)** HeLa S3 cells were synchronized at the G_1-S transition by a double-thymidine block. After release from arrest, extracts were prepared at various times up to 12 hours. The bottom two panels show the amounts of hSecurin and cyclin B1 analyzed by protein immunoblotting. The top graph indicates the percentage of cells in the G_1, S, and G_2-M phase of the cell cycle at the corresponding time points, as determined by FACS analysis. **(B)** Both xSecurin and xSecurin^{dm} protein were translated in vitro in the presence of [^{35}S]methionine. A portion of the translation mixture (2 μl) was added into interphase or mitotic extracts (7 μl) supplemented with bovine ubiquitin (10 μg). The reaction was incubated at room temperature for the time (minutes) indicated below the autoradiograph. **(C)** In vitro–translated xSecurin (1.5 μl) was added to mitotic extract (10 μl) supplemented with ubiquitin (10 μg) and incubated for 15 min. As competitors, a purified *Xenopus* cyclin B1 NH_2-terminal fragment (amino acids 1 to 102) and NH_2-terminal fragments lacking the D-box (CycB1-dbΔ) (*34*) were added to the reaction mixture. The final concentrations of competitors are indicated above the autoradiograph. **(D)** The same as in (B), except that *Xenopus* cyclin B1 NH_2-terminal fragments were labeled by iodination, and xSecurin or xSecurin^{dm} were used as competitors.

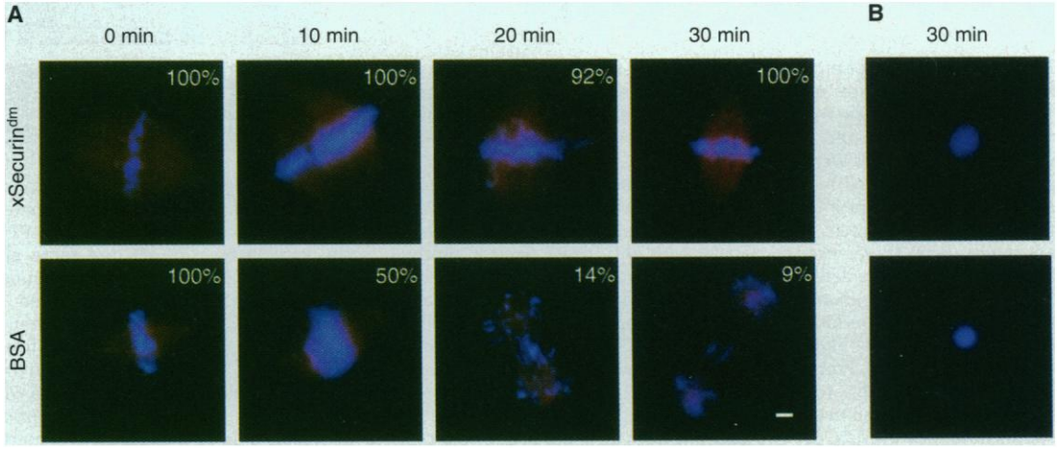

Fig. 3. Inhibition of chromatid separation by *Xenopus* securin. Anaphase was induced in extracts in the presence of **(A)** and in the absence of **(B)** nondegradable Δ90 cyclin B1. Photographs show the Hoechst 33342–stained chromosomes (blue) and rhodamine-labeled mitotic spindle (red) at various times after metaphase release. The percentage of spindles at metaphase for each time point (10 to 25 total spindles) is indicated. The white bar in the lower right panel of (A) represents 10 μm.

(Δ90 cyclin B1) (final concentration, 20 μg/ml). In this system, the cell cycle is arrested at metaphase and can be released into anaphase by addition of calcium. Anaphase movement of chromosomes can be monitored by the positions of the mitotic chromosomes, which were detected by DNA-specific fluorescent dye. We did not observe any differences in interphase nucleus formation, chromosome condensation, or nuclear envelope breakdown between extracts to which xSecurin^{dm} had been added and control extracts. Within 10 min of the second addition of calcium, chromosomes in control extracts had begun to move to the spindle poles (5 out of 10 spindles). No movement was seen in extracts containing xSecurin^{dm} even after 30 min, whereas at the same time in control extracts, 48% (11 out of 23) of the spindles were at late anaphase and 43% (10 out of 23) were at telophase (Fig. 3A).

In budding yeast, Pds1p has been suggested to be part of a checkpoint pathway that arrests the cell cycle at metaphase in the presence of DNA damage that occurs after G_1 (*7*). However, this function of Pds1p may reflect the unique properties of the budding yeast S-phase DNA damage checkpoint. Other eukaryotes, such as fission yeast and vertebrates, arrest the cell cycle at the G_2-M boundary in response to DNA damage occurring after G_1 by inhibiting the activation of the CDC2 cyclin-dependent kinase.

To test whether xSecurin inhibits any aspect of the anaphase progression other than chromatid separation, we performed the above assay with xSecurin^{dm} without the addition of Δ90 cyclin B1 and tested for inhibition of spindle disassembly, chromosome decondensation, and nuclear membrane reformation. No chromatid separation was observed in extracts containing xSecurin^{dm} up to 15 min after the second addition of calcium (eight spindles). Between 15 and 20 min after the second calcium addition, extracts had begun to decondense chromosomes and disassemble spindles. After 25 to 30 min, interphase nuclei were detected in both extracts (Fig. 3B). Protein immunoblot analysis with antibodies to xSecurin and cyclin B1 revealed that cyclin B1 is degraded in the presence of xSecurin^{dm} (*24*). These data demonstrate that xSecurin^{dm} does not interfere with assembly or disassembly of the spindle, with condensation or decondensation of chromosomes, or with breakdown or reformation of the nuclear envelope and thus appears not to interfere with the cycle of CDC2 cyclin-dependent kinase activation and inactivation. Instead, xSecurin specifically inhibits chromatid separation in *Xenopus* egg extracts. It remains possible that the checkpoint pathway is absent in frog embryos and that the vertebrate somatic cells have a checkpoint mechanism involving securins.

The vertebrate securin proteins have been implicated in transformation and tumorigenesis. Overexpression of securins led to the transformation of NIH 3T3 cells, and resulting transformants induced tumors when implanted into nude mice (*22–23*). In addition, expression of hSecurin is high in all carcinoma cell lines that have been tested, and in one case, the levels of hSecurin expression correlate with the malignancy of disease (*29*). The finding that a vertebrate securin has tumorigenic activity is somewhat anticipated because chromosome missegregation has been predicted to be a major source of genetic instability with profound consequences for cancer (*30*). On the basis of its function reported here, the simplest explanation is that tumor formation is the result of aneuploidy caused by defects in the sister-chromatid separation. In yeast, aneuploidy often occurs in mutants defective in sister-chromatid separation (*6, 31, 32*). Chromosome missegregation could lead to increases in the dosage of proto-oncogenes or loss of heterozygosity of tumor suppressors. Alternatively, the tumorigenic activity could result from an unknown function (*21*).

Our results indicate that, despite the low level of conservation among the securins, the basic process of chromatid separation is conserved in all eukaryotes. Identification of human securin as an oncogene suggests that misregulation of chromatid separation may contribute to the generation of malignant tumors.

References and Notes

1. S. Tugendreich, J. Tomkiel, W. Earnshaw, P. Hieter, *Cell* **81**, 261 (1995).
2. R. W. King *et al.*, *ibid.*, p. 279.
3. S. Irniger, S. Piatti, C. Michaelis, K. Nasmyth, *ibid.*, p. 269.
4. S. L. Holloway, M. Glotzer, R. W. King, A. W. Murray, *ibid.* **73**, 1393 (1993).
5. T. Hirano, S. Funahashi, T. Uemura, M. Yanagida, *EMBO J.* **5**, 2973 (1986).
6. A. Yamamoto, V. Guacci, D. Koshland, *J. Cell. Biol.* **133**, 85 (1996).
7. ———, *ibid.*, p. 99.
8. O. Cohen-Fix, J. M. Peters, M. W. Kirschner, D. Koshland, *Genes Dev.* **10**, 3081 (1996).
9. H. Funabiki *et al.*, *Nature* **381**, 438 (1996).
10. R. Ciosk *et al.*, *Cell* **93**, 1067 (1998).
11. H. Funabiki, K. Kumada, M. Yanagida, *EMBO J.* **15**, 6617 (1996).
12. A. Toth *et al.*, *Genes Dev.* **13**, 320 (1999).
13. T. Nagase, N. Seki, K. Ishikawa, A. Tanaka, N. Nomura, *DNA Res.* **3**, 17 (1996).
14. All human genes were cloned by polymerase chain reaction (PCR) from a human fetal thymus cDNA library (Clontech). A fragment of hESP1 cDNA was amplified with a pair of primers (5′-CGGAATTCAATGTCAGAGCCCTCTAAGACTCAG-3′ and 5′-CCCGCTCGAGGGTAGAAAGACCAGTGGCTAC-3′). This cDNA was cloned into the pET28b expression vector to create an NH_2-terminal $(His)_6$ fusion. A 269–amino acid recombinant protein was expressed in *Escherichia coli* according to the protocol provided by the manufacture (Novagen). Recombinant protein was purified up to 90% with Ni–nitrilotriacetic acid (NTA) beads (Qiagen). Full-length hSecurin (or PTTG) was isolated with primers 5′-ATGGCTACTCTGATCTATGTTGATAAGG-3′ and 5′-TTAAATATCTATGTCACAGCAAACAGGTG-3′. The PCR product was then cloned into a modified version of pCS2 for in vitro translation and transfection into mammalian cells. The same fragment was also cloned into a modified pET28a vector to express recombinant protein in *E. coli*. Protein more than 90% pure was obtained by affinity purification with Ni-NTA beads (Qiagen) followed by Resource Q column chromatography. Rabbit polyclonal antibodies to the 269–amino acid hESP1 fragment and full-length hSecurin (or PTTG) were made by Zymed with purified recombinant proteins as antigen. Crude sera were affinity-purified by passing them through affinity AffiGel-10 (Bio-Rad) columns coupled with corresponding antigens. Antibodies were eluted from the affinity-columns by 100 mM glycine (pH 2.5) followed by 100 mM triethylamine (pH 11.5). Affinity-purified antibody to hESP1 (anti-hESP1) cross-reacts with Myc tag. This antibody does not bind to in vitro–translated hSecurin (*24*). The anti-cyclin B1 used in this study was a rabbit antibody purchased from Santa Cruz Biotechnology.
15. E. Harlow and D. Lane, *Antibodies: A Laboratory Manual* (Cold Spring Harbor Laboratory Press, Cold Spring Harbor, NY, 1988).
16. Cells were arrested at metaphase with a thymidine-nocodazole block protocol and at the G_1-S transition with a double-thymidine block protocol (*34*). To determine the cell cycle distribution of each sample, we stained a small portion of the cells with propidium iodide and analyzed them by fluorescence-activated cell sorting (FACS). According to their DNA content, cells were classified as G_1 (N), S (between N and 2N), and G_2-M (2N), and the percentage for each stage of the cell cycle was calculated.
17. Harvested cells were washed with phosphate-buffered saline (PBS) and lysed in 10 volumes of lysis buffer [100 mM KCl, 0.1% NP-40, 20 mM tris (pH 8.0), 2 mM $MgCl_2$, 1 mM EDTA, 1 mM dithiothreitol, and 10% glycerol] supplemented with 1 μM microcystin and leupeptin, pepstatin, and chymostatin (each at 10 μg/ml). Dounce homogenization was used to maximize cell breakage. Cell debris was then removed by ultracentrifugation at 100,000*g* to make high-speed supernatant (S100). For immunoprecipitation, affinity-purified antibodies were covalently coupled onto protein A beads (*14*) at a concentration of about 1 mg/ml. The crude extracts were first incubated with beads coupled to preimmune rabbit immunoglobulin G. Then antibody beads were added into the extract and incubated at 4°C for 3 hours. Unless noted in the text, the beads were washed twice in 100 mM KCl and 0.5% NP-40 wash buffer in the presence of 20 mM tris (pH 8.0), 2 mM $MgCl_2$, 1 mM EDTA, 1 mM dithiothreitol, insulin (0.1 mg/ml), and 10% glycerol (same below); once in 300 mM KCl and 0.5% NP-40 wash buffer; and once in 500 mM KCl and 0.5% NP-40 wash buffer.
18. R. W. King, K. D. Lustig, P. T. Stukenberg, T. J. McGarry, M. W. Kirschner, *Science* **277**, 973 (1997).
19. T. J. McGarry and M. W. Kirschner, *Cell* **93**, 1043 (1998).
20. K. L. Kroll, A. N. Salic, L. M. Evans, M. W. Kirschner, *Development* **125**, 3247 (1998).
21. A. Dominguez *et al.*, *Oncogene* **17**, 2187 (1998).
22. L. Pei and S. Melmed, *Mol. Endocrinol.* **11**, 433 (1997).
23. X. Zhang *et al.*, *ibid.* **13**, 156 (1999).
24. H. Zou and W. M. Kirschner, unpublished observation.
25. Single-letter abbreviations for the amino acid residues are as follows: A, Ala; C, Cys; D, Asp; E, Glu; F, Phe; G, Gly; H, His; I, Ile; K, Lys; L, Leu; M, Met; N, Asn; P, Pro; Q, Gln; R, Arg; S, Ser; T, Thr; V, Val; W, Trp; and Y, Tyr.
26. R. W. King, M. Glotzer, M. W. Kirschner, *Mol. Biol. Cell* **7**, 1343 (1996).
27. H. Funabiki *et al.*, *EMBO J.* **16**, 5977 (1997).
28. C. E. Shamu and A. W. Murray, *J. Cell. Biol.* **117**, 921 (1992).
29. X. Zhang *et al.*, *J. Clin. Endocrinol. Metab.* **84**, 761 (1999).
30. C. Lengauer, K. W. Kinzler, B. Vogelstein, *Nature* **396**, 643 (1998).
31. J. T. McGrew, L. Goetsch, B. Byers, P. Baum, *Mol. Biol. Cell* **3**, 1443 (1992).
32. S. Uzawa, I. Samejima, T. Hirano, K. Tanaka, M. Yanagida, *Cell* **62**, 913 (1990).
33. Extract prepared from nocodazole-arrested HeLa S3 cells was fractionated on a Resource Q column with

a KCl concentration gradient from 100 mM to 1 M in the lysis buffer. Human ESP1 was eluted at about 250 mM KCl. Fractions containing hESP1 were pooled and loaded onto a Superdex 200 column.
34. G. Fang, H. Yu, M. W. Kirschner, *Mol. Cell* **2**, 163 (1998).
35. We thank C. Pfleger and S. Rankin for comments on the manuscript; G. Fang, H. Yu, and other members of the Kirschner laboratory for helpful discussion and technical assistance; C. Pfleger and E. Lee for providing modified pCS2 and pET28a vectors; and Q. Zang for mammalian cell transfection. H.Z. is a fellow of The Jane Coffin Childs Memorial Fund for Medical Research. T.J.M. was supported by a Physician Postdoctoral Grant from the Howard Hughes Medical Institute and a Mentored Clinical Scientist Development Award from the National Heart, Lung, and Blood Institute. Supported by grants GM39023 and GM26875 from NIH awarded to M.W.K.

31 March 1999; accepted 18 May 1999

Different Trajectories of Parallel Evolution During Viral Adaptation

H. A. Wichman,[1]* M. R. Badgett,[2] L. A. Scott,[1] C. M. Boulianne,[1] J. J. Bull[2,3]

The molecular basis of adaptation is a major focus of evolutionary biology, yet the dynamic process of adaptation has been explored only piecemeal. Experimental evolution of two bacteriophage lines under strong selection led to over a dozen nucleotide changes genomewide in each replicate. At least 96 percent of the amino acid substitutions appeared to be adaptive, and half the changes in one line also occurred in the other. However, the order of these changes differed between replicates, and parallel substitutions did not reflect the changes with the largest beneficial effects or indicate a common trajectory of adaptation.

The wealth of molecular data now available reveals that genetic variation is virtually ubiquitous not only between species but also within species. Yet the extent to which this variation is adaptive is enigmatic. This question has taken on new importance as molecular data find increasing use to deduce the mechanism of drug resistance, monitor pathogen populations for incidence of resistance, and compare molecular responses to different drugs and treatment regimes. DNA sequence comparisons are commonly used to address this question, because they carry legacies of their histories that may reflect adaptive change. For example, historical occurrences of adaptive evolution can sometimes be recognized by the high rate of nonsynonymous to synonymous substitution in coding regions, which is a statistical landmark adaptive change (*1*–*4*). However, for two reasons, this statistical approach may be less useful for looking at contemporary adaptation of pests and pathogens. First, adaptive responses to strong selection may require too few changes at the molecular level to leave such "statistical tracks." Second, these methods reveal the occurrence but not the identity of adaptive changes. Parallel evolution—the same change having evolved repeatedly and independently—is also regarded as evidence of adaptation and can reveal the identity of at least some adaptive amino acid substitutions (*5*–*8*). In fact, parallel evolution is a standard criterion used to identify the amino acid substitutions responsible for drug resistance. Although some believe that organisms have too many degrees of freedom to allow this type of predictability, it is not out of the question that the short-term course of adaptation in response to specific selective agents can be predicted, and the short-term course is the one most relevant to human health and infectious disease. It is thus important to determine the extent to which parallel evolution allows us to predict the mechanisms and dynamics of evolution. Here we assess the genomewide dynamics of evolution to examine the molecular basis for and process of adaptation in a viral population under strong selection.

The single-stranded DNA bacteriophage ϕX174 was adapted to high temperature and a novel host (*Salmonella typhimurium*) in a two-stage chemostat for about 1000 population doublings over 10 days. Methods were as described (*9*) except that the temperature was 43.5°C throughout the 10 days of selection.

To guard against contamination, which could be misinterpreted as parallel evolution, we grew replicate lineages in our geographically separated laboratories; we refer to them as the TX and ID replicates. The chemostats were sampled every 24 hours, and isolates from these daily samples were archived into microtiter plates for later analysis. Population sizes in the chemostats were typically in excess of 10^7 except during the first few days of the TX chemostat, when population sizes were closer to 10^4. Our goal was to observe the process of adaptation in a very strong selective environment rather than to dissect responses to specific conditions in the environment. These conditions—large population size and strong selection—are highly favorable to adaptation.

In previous experiments (*9*), we found that adaptation to these conditions resulted in over a dozen substitutions genomewide, with 25 to 50% of them occurring in parallel between any two replicates. On the basis of this parallel evolution alone, we concluded that substitutions were adaptive at more than one-third of the sites where differences were detected. However, the underlying dynamics of evolution and the extent of genetic differentiation within populations was unknown. At one extreme, substitutions might quickly sweep through the population to fixation, so that most genotypes in the population are very similar at any point in time; at the other extreme, there could be multiple competing genotypes present throughout the history of the population. Furthermore, it is not known to what extent high levels of parallel evolution are a signature of similarity of adaptation at the phenotypic level.

Adaptation to chemostat conditions was evident by massive improvements in phage growth rates at the high temperature (Fig. 1). Phage population growth rates were measured as doublings of phage concentration per hour at 43°C under defined conditions (*9*); this assay measures a major component of fitness in the chemostat but does not measure all relevant fitness components. The population growth rate of the ID replicate increased from −5 to 7.1 over the course of the 10 days of selection, with no gain detectable after day 4. This corresponds to a 4000-fold improvement in the number of descendants per hour. The population growth rate of the TX replicate increased from −5 to 12.5 (about 18,000-fold) over the course of the 10 days of selection, with major improvements at several time points. A difference in correlated response to selection was also detected: ID lost its ability to plate on *Escherichia coli* C, whereas TX retained this ability. From this fitness evidence alone, it is obvious that both replicates accumulated changes but that they followed at least somewhat different pathways.

The genetic basis of adaptation was studied at both a nucleotide level and a population level over time. To identify substitutions at high frequency at the end of selection, we obtained complete genome sequences from polymerase chain reaction products amplified

[1]Department of Biological Sciences, University of Idaho, Moscow, ID 83844, USA. [2]Department of Zoology and [3]Institute of Cellular and Molecular Biology, University of Texas, Austin, TX 78712, USA.

*To whom correspondence should be addressed. E-mail: hwichman@uidaho.edu